Nano Research 2015, 8(1): 23–39
DOI 10.1007/s12274-014-0591-z
Review Article

ISSN 1998-0124
CN 11-5974/O4

A mini review of NiFe-based materials as highly active oxygen evolution reaction electrocatalysts

Ming Gong and Hongjie Dai (✉)

Department of Chemistry, Stanford University, Stanford, CA 94305, USA

Received: 13 September 2014
Accepted: 18 September 2014

KEYWORDS

oxygen evolution reaction,
electrocatalysis,
nickel-iron,
water splitting

ABSTRACT

Oxygen evolution reaction (OER) electrolysis, as an important reaction involved in water splitting and rechargeable metal–air batteries, has attracted increasing attention for clean energy generation and efficient energy storage. Nickel/iron (NiFe)-based compounds have been known as active OER catalysts since the last century, and renewed interest has been witnessed in recent years on developing advanced NiFe-based materials for better activity and stability. In this review, we present the early discovery and recent progress on NiFe-based OER electrocatalysts in terms of chemical properties, synthetic methodologies and catalytic performances. The advantages and disadvantages of each class of NiFe-based compounds are summarized, including NiFe alloys, electrodeposited films and layered double hydroxide nanoplates. Some mechanistic studies of the active phase of NiFe-based compounds are introduced and discussed to give insight into the nature of active catalytic sites, which could facilitate further improving NiFe based OER electrocatalysts. Finally, some applications of NiFe-based compounds for OER are described, including the development of an electrolyzer operating with a single AAA battery with voltage below 1.5 V and high performance rechargeable Zn–air batteries.

1 Introduction

The increasing demand for energy and diminishing natural energy resources have led to a revolutionary era of discovering earth-abundant energy alternatives and designing efficient energy-storage devices [1–7]. Hydrogen (H_2), with its high mass-specific energy density, has been considered to be a promising energy source and a substitute for fossil fuels [8–10]. Currently H_2 production still mostly relies on the fossil fuel industry and suffers from low purity and high cost [8]. One of the most efficient ways of producing H_2 at low cost and high purity is water splitting into hydrogen and oxygen by electricity or sunlight [2, 3, 6, 11–16]. The oxygen evolution reaction (OER), as an important half-reaction involved in water splitting, has been intensely investigated for decades [11, 17–20]. OER is a demanding step that includes four proton-coupled electron transfers and oxygen–oxygen bond formation, so it is kinetically not favored and requires a catalyst to

Address correspondence to hdai@stanford.edu

expedite the reaction [21, 22]. Iridium dioxide (IrO_2) and ruthenium dioxide (RuO_2) are the state-of-the-art OER electrocatalysts with low overpotential and Tafel slope, especially in acidic conditions [6, 23–25]. Nevertheless, these catalysts suffer from scarcity and high cost, and cannot be utilized in water splitting industries to obtain economic H_2 energy resources.

Nickel (Ni) is an earth-abundant first row transition metal with corrosion resistance and good ductility. Ni and its oxide were discovered to exhibit electrocatalytic activity towards OER in alkaline solution in the early last century [26, 27]. One of the most interesting discoveries was that nickel is always found in combination with iron (Fe) on earth and Fe impurities in the nickel hydroxide ($Ni(OH)_2$) electrodes can cause detrimental effects on Ni-based alkaline batteries by greatly lowering the OER overpotential [28–32]. The discovery had inspired many scientists to study the phenomenon, optimizing Fe content and synthesizing various NiFe mixed compounds in order to obtain better OER electrocatalysts [33–35]. Up to now, the catalyst utilized in the water electrolysis industry is stainless steel, which is often an alloy consisting of nickel, iron and chromium [13, 36–38]. Recently, with the rising demand for clean and renewable energy, researchers have revisited the field and designed more advanced NiFe-based OER electrocatalysts with higher catalytic activity for efficient and durable water electrolysis.

In this review, we will summarize the discovery and recent progress of NiFe-based compounds for OER electrocatalysis in terms of synthesis, catalytic performance, application and mechanism. We will start with a brief introduction about OER electrocatalysis followed by a summary of the discovery and early optimization strategy of NiFe-based OER electrocatalysts. Then, recent progress on some advanced NiFe-based materials will be reviewed according to their chemical structures, synthetic methods and catalytic activities. Further, some insight into the mechanism of OER electrocatalysis by NiFe compounds and possible future directions to improve the performance NiFe OER electrocatalysts will be discussed. Finally, the applications of NiFe-based OER catalysts including water splitting and rechargeable metal–air batteries will be briefly introduced. Through this review, we hope to provide the readers with a distinct perspective of the history, present and future of this field.

2 OER electrocatalysis

Water oxidation or OER is a reaction generating molecular oxygen through several proton/electron-coupled processes [39, 40]. In acidic conditions, the reaction operates through oxidation of two water molecules (H_2O) to give four protons (H^+) and one oxygen molecule (O_2) by losing a total of four electrons [40]. In basic conditions oxidation of hydroxyl groups (OH^-) takes the lead, and they are transformed into H_2O and O_2 with the same number of electrons being involved [39].

$$\begin{aligned} 2H_2O &\longleftrightarrow 4H^+ + O_2 + 4e^- \\ 4OH^- &\longleftrightarrow 2H_2O + O_2 + 4e^- \end{aligned} \quad (1)$$

As OER is an electron-coupled uphill reaction, electricity is usually used as energy input to drive the reaction. The standard potential for OER at pH 0 (as shown in Eq. (1) when the concentration of H^+ is 1 M) is 1.23 V vs. the normal hydrogen electrode (NHE). As the reaction involves H^+ or OH^-, the potential is dependent on pH by shifting 59 mV for each pH unit increase according to the Nernst equation,

$$E = E^{\circ} - \frac{RT}{nF}\ln\frac{[\text{Red}]}{[\text{Ox}]} \quad (2)$$

(E is the cell potential, E° is the cell potential at standard conditions, R is the ideal gas constant, T is the temperature in Kelvin, n is the number of moles of electrons involved each mole of reaction, F is the Faraday constant, [Red] is the concentration of reduced molecules and [Ox] is the concentration of oxidized molecules).

To remove the impact of pH on the applied potential, researchers have introduced a reversible hydrogen electrode (RHE) reference by taking into account the pH shift, and thus the theoretical potential required for OER is always 1.23 V vs. RHE at all pHs. As shown in Eqs. (1) and (2), generation of each O_2 molecule requires a transfer of four electrons, and as multiple electron transfer at one time is not kinetically

favorable, OER usually involves multiple steps with one electron transfer per step [39]. An accumulation of the energy barrier in each step leads to the sluggish kinetics of OER with large overpotential to overcome. Therefore OER electrocatalysis is desired to expedite the reaction and lower the potential. As very few non-precious metal oxides can survive under oxidative potentials in acidic condition [24], researchers have been searching for non-precious metal-based candidates for OER electrocatalysis in alkaline conditions, in which most metal oxides or hydroxides are chemically stable. An ideal OER electrocatalyst should have low overpotential, high durability, low-cost, high earth-abundance and scalability. However, up to now catalysts meeting these requirements have not yet been discovered. NiFe-based compounds are one of the most promising candidates, showing the highest OER electrocatalytic activities among all non-precious metal-based electrocatalysts.

3 Early discovery

The poisoning effect of Fe impurities on the $Ni(OH)_2$ electrodes in alkaline batteries were first found by Edison and Junger soon after their discovery of Ni-based alkaline batteries. Systematic studies of the role of iron contamination revealed that increasing the iron contamination degree led to decreasing capacity and cycle life of the alkaline batteries by lowering the OER overpotential [28–32]. Such an effect could be observed with concentrations below 1% Fe and was attributed to the catalytic behavior of the conducting ferric oxide in the study by Mlynarek et al. [35]. With the rising interest in water splitting in the 1980s, Corrigan et al. first studied the oxygen evolution behavior of nickel oxide electrodes with Fe impurities. Fe impurities from the electrolyte co-precipitated onto the nickel oxide films were discovered to have similar strong effects in catalyzing oxygen evolution reactions [34]. The decrease in OER overpotential and decrease in discharge capacity was reported even at an ultra-low Fe concentration (0.01%) (Fig. 1), demonstrating the high sensitivity nature of OER on Ni-based electrodes to Fe impurities. By adjusting the Fe content, a composite NiFe hydrous oxide with >10% Fe showed intriguing activities toward OER electrocatalysis with ~200–250 mV overpotential at a current density of 10 mA/cm^2 and a low Tafel slope of 20–25 mV/decade (Fig. 1(b)). In addition, Corrigan et al. also introduced

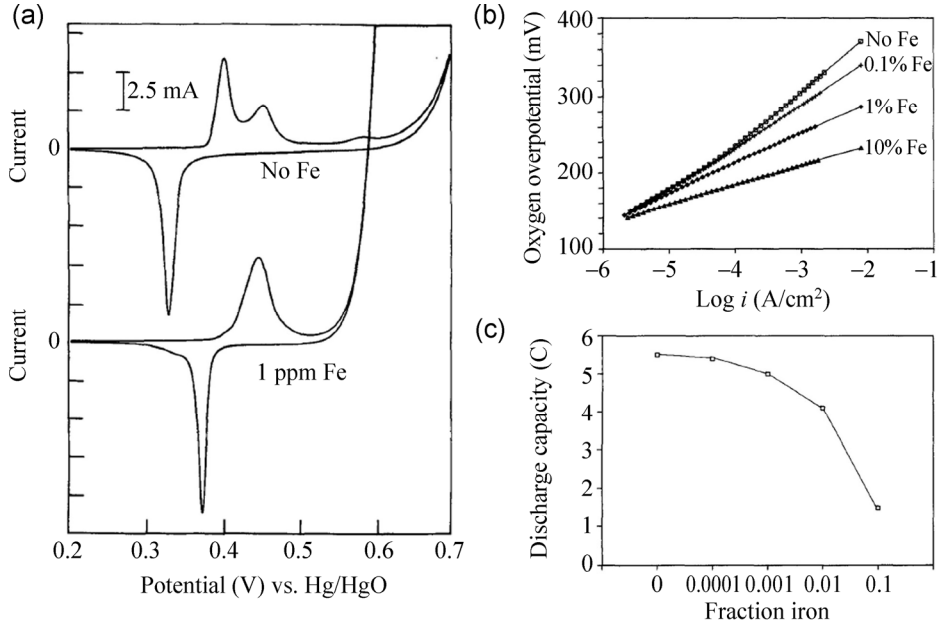

Figure 1 (a) Effect of iron impurities in the electrolyte on nickel electrodes studied by cyclic voltammetry at a scan rate 10 mV/s. (b) Tafel plots of oxygen evolution at thin nickel oxide film electrodes with different amounts of coprecipitated iron by open-circuit decay measurements. (c) Effect of coprecipitated iron on the discharging capacity of at thin nickel oxide film electrodes at a discharge current density of 8 mA/cm^2. Reproduced with permission from Ref. [34], Copyright © 1987 The Electrochemical Society.

other metal ions into $Ni(OH)_2$ films by electrodeposition and the film with co-deposited $Fe/Ni(OH)_2$ exhibited high OER electrocatalytic activity to afford a 287 mV overpotential at 16 mA/cm^2, outperforming all other d and f block metals except cerium. These results suggested a promising future for NiFe-based compounds in low-cost OER electrocatalysis [41].

4 NiFe alloy

The affinity of Ni (atomic number 28) and Fe (atomic number 26) facilitates the formation of a NiFe alloy, as indicated by steel and abundance of NiFe alloy in the earth's core. One of the most facile methods of synthesizing NiFe-based electrocatalysts is to mechanically mix metallic Ni and Fe to give an NiFe alloy. For example, amorphous Ni–Fe–Si–B alloys prepared by melt spinning on a CuZr drum showed an OER potential of ~700 mV vs. mercury/mercury oxide reference electrode (Hg/HgO) (~340 mV in overpotential) at 100 mA/cm^2 in 30 wt.% potassium hydroxide (KOH) at room temperature [42]. Later work demonstrated the synthesis of various combinations of cobalt, nickel, molybdenum and iron alloys by mechanical alloying. The alloys showed improved OER electrocatalytic activity, giving current densities of 11–234 mA/cm^2 at an overpotential of 400 mV at different temperatures of 298 K, 323 K and 343 K [43]. The mechanical alloying process is a good approach for mixing a wide range of elements to study the synergistic effects on different elements, but the nature of the physical mixture leads to large crystal size with low electrochemically accessible surface area and lack of chemical contact between different elements. The inability to produce novel chemical structures by physical alloying limits its potential in exploring novel structures for OER electrocatalysis.

An alternative way of synthesizing NiFe alloy is by cathodic electroreduction of mixed metal salt solutions. Since nanoscale NiFe alloy is often converted into NiFe oxide when exposed to air, especially at the surface, the catalyst has sometimes been reported as electrodeposited NiFe oxide. Such an approach can afford optimal adherence of the active catalytic material to the underlying substrate, thereby lowering the overpotential introduced by ohmic loss. By tuning the electrolyte composition and electrodeposition parameters such as current and time, NiFe alloys with a variety of morphologies and catalytic properties can be synthesized. Potvin and Brossard first reported a citrate solution with a metal sulfate salt as the electrolyte and derived a particle-based film of NiFe alloy early in 1992 [44]. Among the films with different Ni/Fe ratios, the 45/55 at.% Ni–Fe deposits showed the best performance with a current density of 351 mA/cm^2 at an overpotential of 350 mV in 40 wt.% KOH at 80 °C. Both the cathodic electrodeposition condition and pre-anodization conditions were found to greatly influence the OER catalytic activity, suggesting the possibility of improving catalyst performance by fine-tuning the electrosynthesis conditions. Ascorbic acid [45], boric acid [46–50] and ammonium sulfate [24, 51–54] solutions containing iron and nickel sulfate were later discovered as suitable electrolytes for cathodic electrodeposition of NiFe films, and recently the latter two electrolytes have been widely used for NiFe alloy electrosynthesis. Grande and Talbot studied the NiFe thin films electrodeposited in an electrolyte containing boric acid, and addition of boric acid solutions was found to be essential for NiFe co-deposition by decreasing the rate of Ni deposition while increasing the rate of Fe deposition [46]. As appropriate Fe content was earlier demonstrated to be a significant factor impacting the OER electrocatalytic activity, and increasing Fe content by the boric acid approach could potentially improve the activity as confirmed by later studies finding excellent electrocatalytic activity with uniform NiFe films deposited in a boric acid solution [47–50]. Merrill and Dougherty further explored an ammonium sulfate solution for NiFe electrodeposition and they compared the catalyst with other mixed transition metal deposited in similar conditions [54]. The as-synthesized NiFe film outperformed other catalysts by at least 50 mV with an incredibly low Tafel slope of 14.8 mV/decade, corroborating the highly active nature of NiFe-based materials for OER catalysis. By adopting similar synthetic approach, Louie and Bell optimized the Ni/Fe ratio and the NiFe catalyst containing 40% Fe exhibited the highest activity among the catalyst [53]. *In situ* Raman spectroscopy of the deposited NiFe film elucidated the correlation between the average Ni

oxidation state and the OER catalytic activity, which will be discussed later in the review.

In addition, the synthetic method of electrodeposition in ammonium sulfate was further utilized in McCrory et al.'s study of evaluating the activities of a series of heterogeneous electrocatalyst benchmarks [24]. In concentrated alkaline conditions of 1 M sodium hydroxide (NaOH), NiFe-based compound stood out among all non-precious metal catalysts with nearly 10 times higher activity per electrochemically active surface area and stable catalytic behavior over 2 hours, suggesting useful NiFe-based electrocatalysts for OER catalysis applications (Fig. 2). The ease of NiFe alloy synthesis by electrodeposition and the excellent

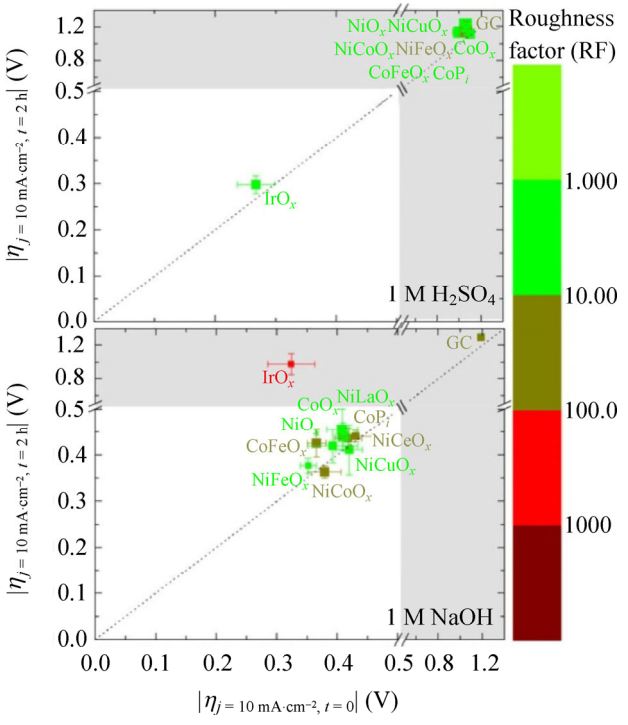

Figure 2 Comprehensive plots of catalytic activity, stability, and electrochemically active surface area for a variety of OER electrocatalysts in acidic (top, 1 M H_2SO_4) and alkaline (bottom, 1 M NaOH) conditions. The *x*-axis depicts the overpotential at 10 mA/cm^2 (geometric area) at time t = 0, and the *y*-axis depicts the overpotential at 10 mA/cm^2 (geometric area) at time t = 2 h. A stable catalyst should fall on the diagonal dashed line of the plot, and an active catalyst should be on the bottom left of the plot. The color of each point represents the roughness factor (RF) of the catalyst with light green representing RF = 1, and dark red representing RF > 10^3. The unshaded white region is the region of interest for screening the catalysts where the overpotentials at 10 mA/cm^2 (geometric area) at both time t = 0 and 2 h are <0.5 V. Reproduced with permission from Ref. [24], Copyright © 2013 American Chemical Society.

adherence to the substrate makes it a popular approach for studying NiFe-based compounds. However, the limitation of NiFe alloy is that structural transformation is needed before entering an OER active phase. Such structural evolution is often confined to the surface where the electrolyte is accessible, implying the necessity of NiFe deposits with high surface area for further improving the catalyst. Even though some recent studies demonstrated the electrodeposition of dendritic NiFe alloys with high OER performance [55], few reports have been dedicated to highly porous NiFe films with large surface area. In addition, it still remains unclear whether the oxidation of the NiFe film fully penetrated through the entire film or only occurred on the surface, posing a challenge to structural analysis both on the surface and beneath the surface in determining the active phase for OER electrocatalysis.

5 NiFe oxide

Unlike the metallic state of Ni and Fe element in NiFe alloy, NiFe oxide often has oxidation states of +2 and +3 for Ni and Fe respectively, which are much closer to the oxidation states in the OER region. To derive the NiFe oxide phase, annealing at high temperature is usually required and therefore most NiFe oxides are crystalline with well defined structure [56–63] (often with X-ray diffraction analysis). NiFe oxide can be prepared by a variety of synthetic methods. The earliest approach was by reactive sputtering co-deposition with a NiFe alloy target and a 20% oxygen/argon atmosphere with 10 mTorr pressure [64]. Tremendously improved activity by Fe incorporation into Ni oxide films was obtained, and the best sputtered sample exhibited a current density of 80 mA/cm^2 at an overpotential of 362 mV with a Tafel slope of less than 40 mV/decade. Importantly, due to the crystalline nature of the sputtered NiFe oxide, an impressive durability of over 7,000 hours was observed [64].

With a Ni/Fe ratio of 1:2, the NiFe oxide can form nickel ferrite ($NiFe_2O_4$) with a spinel structure, showing cubic closed-packed oxide anions with Ni^{2+} occupying one-eighth of the tetrahedral holes and Fe^{3+} occupying half of the octahedral holes. Owing to the highly corrosion-resistant nature (insoluble in most acids),

nickel ferrite has attracted much attention as an OER electrocatalyst, even though it is more often investigated as a magnetic material due to its strong magnetism [65, 66]. The nickel ferrite catalyst can be produced through low-temperature precipitation followed by high temperature annealing. Some earlier studies gave similar conclusions, namely that the NiFe mixed compound (spinel $NiFe_2O_4$) outperforms Fe alone (spinel Fe_3O_4) and Ni alone (cubic NiO) in OER electrocatalytic activity [61]. Due to the wide variety of possible spinel structures, researchers have recently focused on substituting the $NiFe_2O_4$ by other cations (e.g., Cr, V, Mo and Co) in order to enhance the electrocatalytic activity [56–59]. Even though improved OER activities were observed, the $NiFe_2O_4$ or other crystalline NiFe oxide catalysts seem to underperform the electrodeposited NiFe films, probably due to the rigidity of the crystalline NiFe oxides.

Though most NiFe oxide are crystalline as a result of high temperature annealing, one exception is the production of amorphous NiFe oxide by thermal decomposition of metal–organic compounds at relatively low temperatures. Smith et al. introduced a facile photochemical metal–organic deposition (PMOD) method for preparing amorphous (mixed) metal oxide thin films with thickness of 150 to 200 nm (Fig. 3(a)) [67]. Interestingly, amorphous films synthesized at 100 ˚C were found to have better OER electrocatalytic performance than crystalline films formed at 600 ˚C (Fig. 3(d)). By comparing various oxide films synthesized by the same PMOD method, mixed NiFe oxide and mixed oxide containing Ni and Fe were confirmed to outperform other catalysts with low overpotential and low Tafel slope (Figs. 3(b)–3(d)).

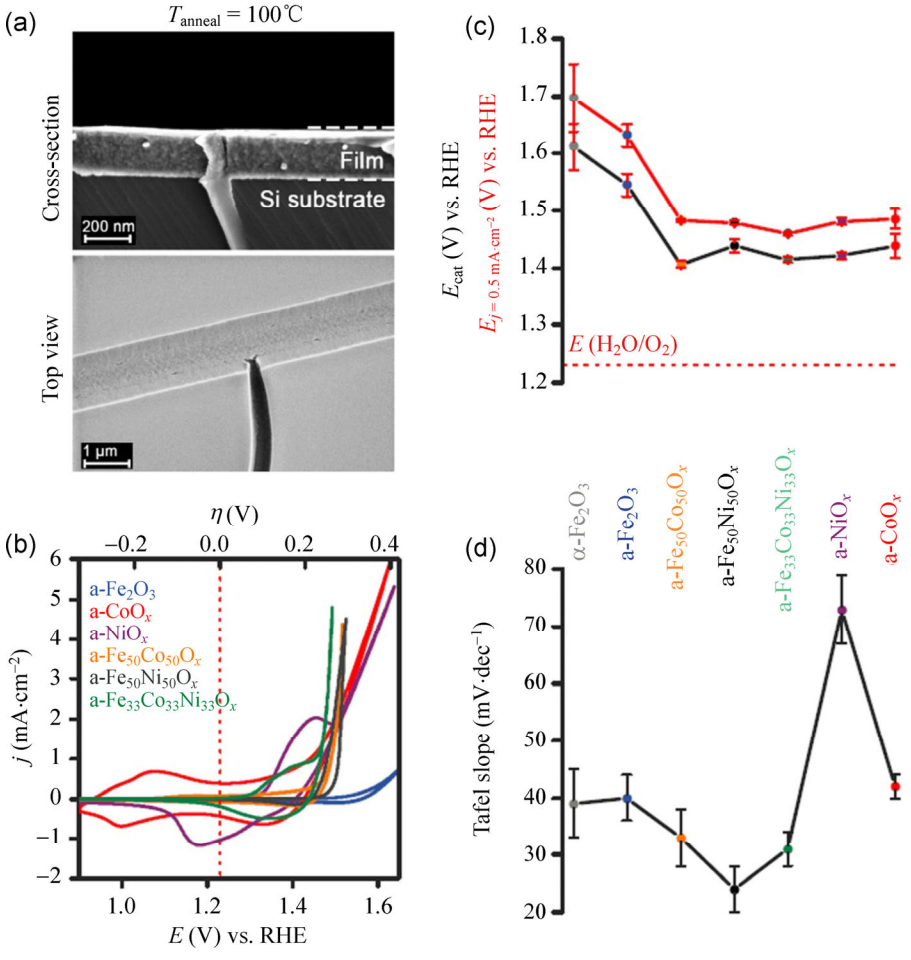

Figure 3 (a) Cross-section and top-down SEM image of the amorphous Fe_2O_3 film formed by PMOD by annealing at 100 ˚C in air for 1 hour. (b) Cyclic voltammograms at a scan rate of 10 mV/s. (c) Overpotentials at 0.5 mV/cm^2 (geometric area). (d) Tafel slopes of different oxide films prepared by PMOD in 0.1 M KOH. Reproduced with permission from Ref. [67], Copyright © 2013 American Association for the Advancement of Science.

However, the catalyst tended to decay slowly over time, probably due to its amorphous nature. Therefore, the balance between good crystallinity—to obtain high durability with rigid structures under OER operation—and amorphousness—to obtain high activity with large electrochemically active surface area (ECSA)–is essential for developing advanced NiFe-based OER electrocatalysts.

6 NiFe layered double hydroxides

Layered double hydroxides (LDH) are a class of layered materials consisting of positively charged layers and charge-balancing anions in the interlayer region [68–70]. The positively charged layers are constructed by partially substituting divalent cations (e.g., Ni^{2+}, Mg^{2+}, Ca^{2+}, Mn^{2+}, Co^{2+}, Cu^{2+}, Zn^{2+}) or monovalent cations (e.g., Li^{+}) by trivalent cations (e.g., Al^{3+}, Co^{3+}, Fe^{3+}, Cr^{3+}). The intercalated anions are typically carbonate (CO_3^{2-}), but this can easily be replaced by other anions (e.g., NO_3^-, SO_4^{2-}, Cl^-, Br^-). Therefore, the LDH structure is attractive for use in electrochemical processes as it is highly accessible to electrolytes by anion exchange. The synthesis of NiFe LDH was achieved in earlier studies [71, 72], but NiFe LDH for oxygen evolution electrocatalysis has been barely studied until recently. One of the major issues associated with NiFe LDH is its low conductivity, a common problem with hydroxides [73]. Researchers have attempted to solve the problem by either hybridizing it with a conductive material or directly growing LDH on conductive substrate [73–76].

Our group was the first to develop a NiFe LDH with or without carbon nanotubes as support for OER electrocatalysis (Fig. 4(a)) [73]. By slow hydrolysis of a metal salt at low temperature followed by a high-temperature solvothermal step for crystallization, we obtained ultrathin NiFe LDH nanoplates (~5 nm) covalently attached to a multi-walled carbon nanotube (Fig. 4(b)). The hybrid material could deliver a current density of 5 mA/cm^2 at a overpotential of 250 mV with a Tafel slope of 31 mV/decade in 1 M KOH at a loading of 0.25 mg/cm^2 (Fig. 4(c)). The LDH nanoplates alone without nanotubes showed a slightly lower OER catalytic activity by ~30 mV on substrates, due to the relatively low conductivity, but if loaded on highly

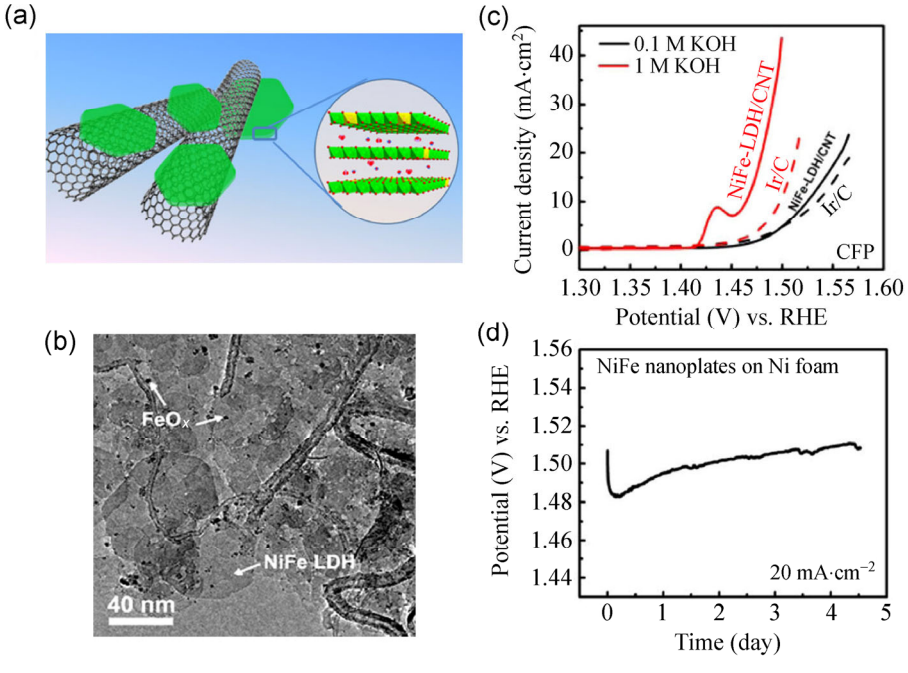

Figure 4 (a) Schematic view of the hybrid architecture and NiFe LDH structure. (b) TEM image of the NiFe-LDH/CNT hybrid. Arrows point to NiFe-LDH plates and iron oxide (FeO_x) particles. (c) iR-compensated polarization curves of NiFe-LDH/CNT hybrid and commercial Ir/C catalyst on carbon fiber paper (CFP) loaded at 0.25 mg/cm^2 for both catalysts electrode in 0.1 and 1 M KOH. (d) chronopotentiometry of NiFe LDH nanoplates without CNT loaded onto Ni foam at a loading of ~5 mg/cm^2 in 1 M KOH with a constant current density of 20 mA/cm^2. Reproduced with permission from Ref. [73], Copyright © 2013 American Chemical Society.

conductive Ni foam, NiFe LDH nanoplates could afford high activity as well as high stability for at least four days (Fig. 4(d)). Therefore, the high performance of the material can be mainly attributed to the LDH phase and further facilitated by the ultrathin nature of nanoplates and strong coupling to carbon nanotubes.

The high intrinsic OER electrocatalytic activity of NiFe LDH was further confirmed by later studies of NiFe LDH grown on graphene [74], carbon quantum dots [75] and Ni foam substrates [76]. To study the active site of NiFe LDHs, Trotochaud et al. systematically studied the effect of Fe incorporation into $Ni(OH)_2$ films (NiFe LDH structure) on OER catalytic activity [77]. Surprisingly, *a* >30-fold increase in conductivity was observed upon Fe incorporation into the $Ni(OH)_2$ film. However, since the recorded *i*–*V* curves were iR-compensated, the conductivity improvement could not explain the OER current boost. A further study of the effect of film thickness on turnover frequency (TOF) showed a lower dependence of thickness for co-deposited Fe films than Fe-free films, suggesting an Fe-induced partial-charge-mechanism. Another important conclusion of the study was that upon aging, $Ni(OH)_2$ could increase its crystallinity as well as collect Fe impurities in the electrolyte [77], illustrating the cause of improved activity of aged $Ni(OH)_2$ films and the high electrocatalytic activity of NiFe LDH phase.

Due to the large interlayer spacing between individual layers in the LDH structure, exfoliation of LDH structure into few layers and single sheets has been demonstrated to expose more surface sites [69]. Song and Hu demonstrated a synthetic route for preparing an exfoliated LDH by an anion exchange step to expand interlayer spacing and a following delamination step in formamide solution (Fig. 5(a)) [78]. The as-synthesized exfoliated LDH nanosheet demonstrated an average thickness of ~0.8 nm, implying single or double layer structures (Fig. 5(c)). Upon exfoliation, significantly higher OER electrocatalytic activity was observed with a variety of LDHs including NiFe LDH (Fig. 5(b)). The authors proposed

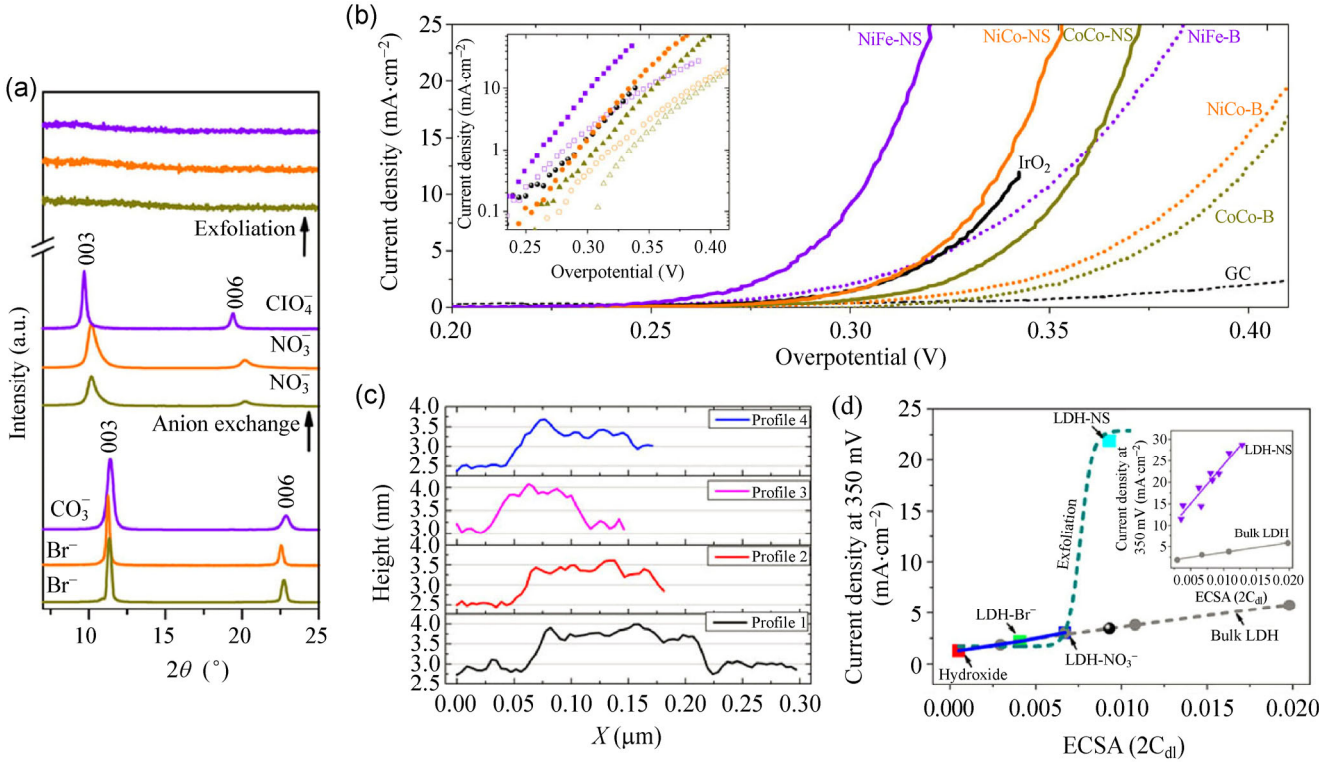

Figure 5 (a) XRD spectra of bulk, anion-exchanged and exfoliated LDH (CoCo LDH: yellow-green; NiCo LDH: orange; NiFe LDH: purple). (b) Polarization curves of bulk and exfoliated LDH at a loading of 0.07 mg/cm^2 in 1 M KOH. IrO_2 nanoparticles were test side-by-side for comparison. The inset shows the Tafel plots. (c) Height profile of the exfoliated NiCo LDH derived from atomic force microscopy (AFM). The average thickness is ~0.8 nm. (d) Current density at an overpotential of 350 mV plotted versus ECSA ($2C_{dl}$) for different NiCo-based materials. Reproduced with permission from Ref. [78], Copyright © 2014 Nature Publishing Group.

that a large number of active sites were exposed after exfoliation, as they observed dramatically improved OER activity with similar ECSAs (Fig. 5(d)). However, further spectroscopy and theoretical calculation studies are needed to confirm the active site of NiFe LDH.

NiFe LDH has recently been demonstrated to possess excellent electrocatalytic activity and durability for OER catalysis; however, the active site of NiFe LDH remains unclear, and further mechanistic studies could help to understand the structural relevance to OER electrocatalytic activity and further improve NiFe LDH-based electrocatalysts by constructing more advanced structures to tune the electronic property.

7 Screening NiFe-based catalysts containing other elements

One straightforward approach to develop NiFe-based electrocatalysts with better activities is to introduce other elements into the structures. However, changing elements and tuning element ratios demand tremendous efforts. Therefore, researchers have designed high-throughput screening methods by O_2 probes to visualize the OER electrocatalytic activity trend while tuning the elements [79–81]. Consequently, more OER catalyst candidates could be screened during a single scan. Gerken et al. utilized fluorescent pressure-sensitive paints that can vary their fluorescence intensity upon detecting different partial pressures of O_2 [79]. Improved quantitative measurements were enabled by two fluorophores with one insensitive to O_2 and the other with fluorescence which was quenched in proportion to the partial pressure of O_2 (Fig. 6(a)). Twenty-one different ternary metal oxide combinations were screened and each ternary oxide measurement contained twenty-one samples with different element ratios. The intensity of each individual point was eventually plotted into a triad showing different OER catalytic activity with different elemental ratios for each ternary oxide measurement. Through comparing different triads, a ternary oxide composed of a combination of 60% Ni/20% Al/20% Fe was demonstrated to exhibit the highest catalytic activity, which is consistent with the high intrinsic activity of NiFe oxide in OER catalysis (Fig. 6(b)). The high OER catalytic activity of the ternary NiAlFe

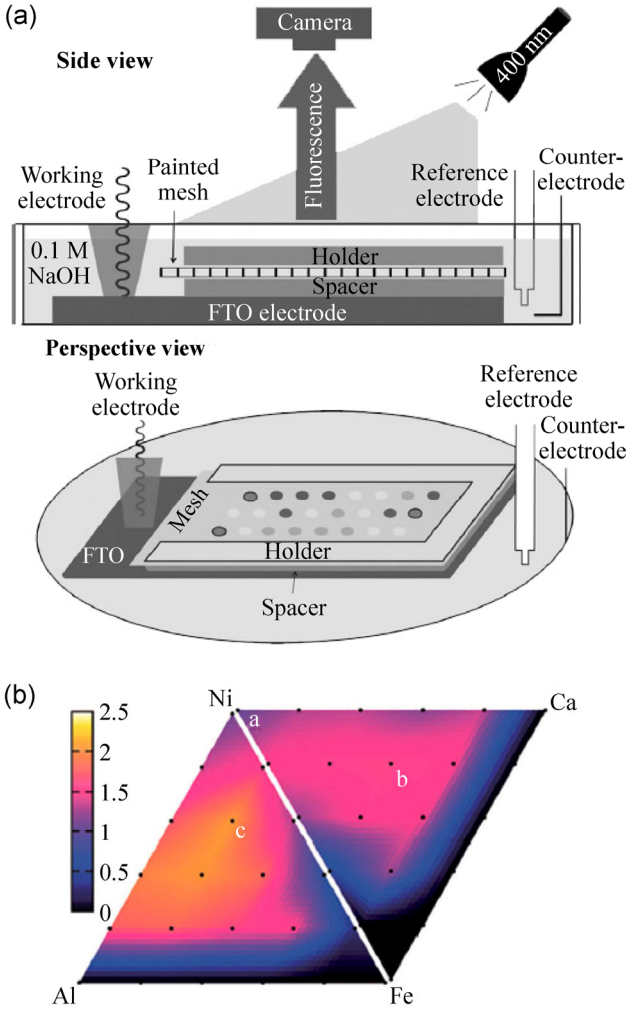

Figure 6 (a) Schematic diagram of the high throughput electrochemical screening apparatus. (b) Activity plot with respect to different composition for the triads Ni/Al/Fe and Ni/Ca/Fe. Reproduced with permission from Ref. [79], Copyright © 2012 WILEY-VCH Verlag GmbH & Co. KGaA, Weinheim.

compound was corroborated by their later studies on inverse spinel $NiFeAlO_4$ structures [82]. The team further improved the throughput by an order-of-magnitude with 15 × 14 rectangular arrays of varied oxide compositions. By screening 3,500 earth abundant mixed oxide catalysts, NiFe oxides containing a third metal (e.g., Al, Ga and Cr) were confirmed to be most active OER catalysts in alkaline conditions [80]. The triads containing ternary oxides were further extended to a quaternary (Ni–Fe–Co–Ce) oxide system, in which 5,456 different compositions were investigated by a similar high-throughput screening method using O_2^- sensitive probes [81]. An interesting pseudo-ternary cross-section containing 665 different compositions

was discovered to possess better catalytic performance than other combinations.

The high throughput screening method provides an efficient and cost-effective way of discovering new OER-catalytic active materials with a variety of element combinations. However, currently only materials with simple synthetic methods can be screened, but advanced OER catalysts might need complicated synthesis under harsh conditions. Therefore, the most efficient way of discovering and designing novel OER catalysts with better performance might be using modern synthetic methodology under the guidance of theoretical calculations and high throughput screening.

8 Mechanism

Even though a variety of NiFe-based catalysts have been developed, the active phase and detailed mechanism for NiFe-based compounds still remain unclear and under debate. The controversy stems from the difficulty of identifying the structure and pathway during OER electrocatalysis, both experimentally and theoretically. The earliest related mechanistic studies involved the active phase of $Ni(OH)_2$ or nickel oxide (NiO_x) catalyzing OER. The phase transformation of $Ni(OH)_2$-based electrode followed the Bode diagram with β-$Ni(OH)_2$ and α-$Ni(OH)_2$ changing into β-nickel oxyhydroxide (β-NiOOH) and γ-NiOOH respectively during charging and discharging. γ-NiOOH can also be derived from overcharging β-NiOOH, while α-$Ni(OH)_2$ is converted into β-$Ni(OH)_2$ after aging [83]. The α-$Ni(OH)_2$/γ-NiOOH pathway generally involves more electron transfer and structural change than the β-$Ni(OH)_2$/β-NiOOH pathway [84]. Over a long period of time, β-NiOOH has been generally considered as the active phase for OER catalysis due to the observation of improved OER catalytic activity after aging [83, 85, 86]. However, recent studies have indicated an active phase of γ-NiOOH. By using *in situ* X-ray absorption near-edge structure (XANES) spectroscopy, a NiOOH thin film deposited from a nickel-containing borate electrolyte was found to exhibit an average oxidation state of +3.6, indicating a predominant portion of γ-NiOOH during OER electrocatalysis [87]. Further, by studying the impact of Fe impurity upon the OER activity of NiOOH films, Trotochaud et al. argued that during aging process the NiOOH film could gradually collect the Fe impurities remaining in the solution with modified electronic properties, which could greatly contribute to the improved activity, thereby challenging the long-held view of a more active β-NiOOH phase [77].

Further studies of the effect of Fe incorporation on Ni-based OER electrocatalysis have been carried out using a number of techniques [e.g., density functional theory (DFT) calculations and *in situ* spectroscopy]. Corrigan and Bendert first attributed the activity gain after Fe incorporation to the improvement in electrical conductivity [34]. The better conductivity was later confirmed by steady state *in situ* film conductivity measurements, but the huge overpotential difference at low current densities cannot be explained by a more conducting Fe-incorporated film [77]. Also, the iR-compensation usually adopted in most of the electrocatalysis studies could minimize the impact of conductivity on OER catalytic performance.

Different types of *in situ* spectroscopy have recently attracted increasing attention as useful tools for probing the catalyst while operating under catalytic conditions. *In situ* extended X-ray absorption fine structure (EXAFS) revealed that under OER conditions the average coordination number of Fe atoms increases, corroborating the participation of Fe in enhancing OER catalytic activity [88]. Based on the crystalline $NiFe_2O_4$ phases observed by X-ray diffraction (XRD) as well as the high coordination number of octahedrally coordinated Fe in $NiFe_2O_4$, $NiFe_2O_4$ was postulated as the active phase. The possibility of other NiFe-based compounds formed by *in situ* electrochemical oxidation (especially at the surface) contributing to the activity cannot be fully ruled, however, out due to the mostly amorphous nature of the electrochemically synthesized materials.

The identification of $NiFe_2O_4$ as the active phase was later challenged by Louie and Bell using *in situ* Raman spectroscopy [53]. Raman spectra of the NiFe oxide films under bias exhibited no traces of $NiFe_2O_4$ (which has typical bands at 700 cm^{-1}), implying that no $NiFe_2O_4$ was formed at the surface under oxidative potentials (Fig. 7(a)). The polarized NiFe oxide films showed typical Raman peaks of NiOOH at 475 cm^{-1}

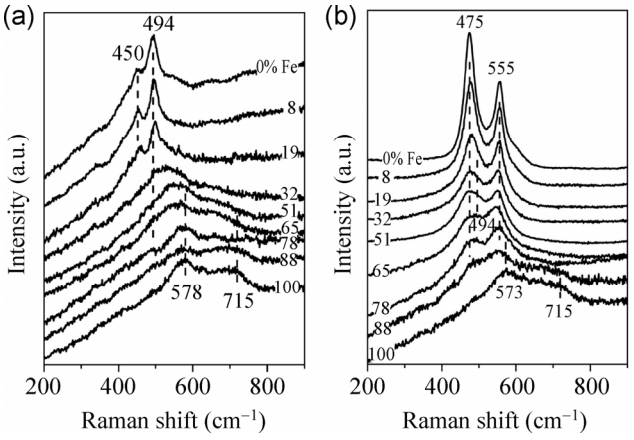

Figure 7 *In situ* Raman spectra of Ni–Fe catalysts with different composition in 0.1 M KOH at a potential of (a) 0.2 V vs. Hg/HgO (1 M KOH) and (b) 0.6 V vs. Hg/HgO (1 M KOH). Reproduced with permission from Ref. [53], Copyright © 2013, American Chemical Society.

and 555 cm^{-1} even at Fe contents of 90% or higher, indicating that NiOOH is a possible active phase in OER electrocatalysis, even in the presence of Fe (Fig. 7(b)). Additionally, the Ni–O environment in NiFe oxide without bias was dramatically modified by Fe incorporation, especially at higher Fe contents. Broader peaks with higher degrees of disorder were observed at high Fe/Ni ratios (Fig. 7(b)). Such structural modification after introduction of Fe might be responsible for the improved OER activity.

DFT calculations have been widely employed as a predictive or supporting tool for various electrochemical processes, but few theoretical studies have focused on Ni-based or NiFe-based materials for OER electrocatalysis. Recently, Li and Selloni performed spin-polarized DFT calculations on different combinations of Ni and NiFe oxides [89]. An activity trend of Fe-doped β-NiOOH (0.26 V) > $NiFe_2O_4$ > β-NiOOH > Fe-doped γ-NiOOH > γ-NiOOH > Fe_3O_4 was obtained by calculating the overpotential required for OER. The Fe-doped β-NiOOH even possessed a theoretically better activity than RuO_2, a well-known OER catalyst. Nevertheless, one limitation of this study was that the activity trend was calculated using the elemental steps of OER in acidic conditions involving four proton-coupled electron transfers. The NiFe-based materials were demonstrated as highly active catalysts in basic conditions, which proceeded through electron transfers from hydroxyl groups to water molecules with the release of oxygen gas. Therefore, the different pathways could lead to different intermediates and different activity trends. However, it is difficult to carry out DFT calculations on basic systems because the presence of charged intermediates during each elemental step demands tremendous time and effort [12].

Overall, various attempts to understand the mechanism of improved activity with NiFe-based compounds have been conducted by spectroscopic studies and theoretical calculations. A convincing and congruous theory has yet to emerge due to limitations of our knowledge of the structure of NiFe compounds generated *in situ* on the surface, and limitations on calculations when introducing charged intermediates. Further mechanistic studies are still desired in order to shine light on our understanding of OER processes and develop new OER electrocatalysts with better activity.

9 Applications

One of the most important applications for OER is water electrolysis, which is a promising way of producing high-purity hydrogen gas with low cost for hydrogen fuel cell powered electric vehicles with zero emission. Our group recently paired up a NiFe LDH catalyst serving as an oxygen-generating anode and a nickel oxide/nickel hetero-structured catalyst on CNTs (NiO/Ni–CNT) serving as a hydrogen generating cathode in 1 M KOH to make an alkaline electrolyzer (Fig. 8(a)) [12]. The device could achieve a current density of 20 mA/cm^2 at a voltage as low as 1.5 V and a current density of 100 mA/cm^2 at a voltage of 1.58 V at room temperature with both electrodes having a loading of 8 mg/cm^2 (Figs. 8(b) and 8(c)). Further increasing the operating temperature to 60 ℃ greatly enhanced the reaction kinetics and lowered the voltage to 1.4 V (Figs. 8(b) and 8(c)). The low voltage required can enable the device to be powered by a single alkaline AAA battery with gas bubbles evolved on both electrodes (Fig. 8(d)). Notably, this was the first time a voltage <1.5 V has been achieved for electrolyzers with non-precious metal electrocatalysts. With their low-cost, high activity and facile synthesis, the NiFe-based and NiO/Ni-based electrocatalysts

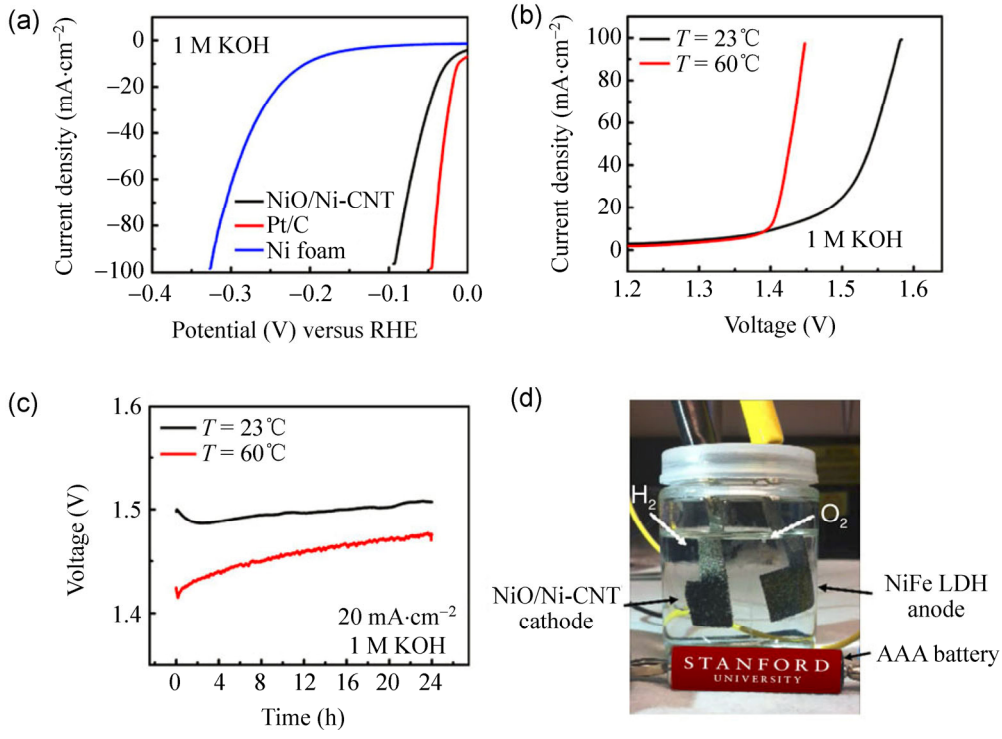

Figure 8 (a) Linear sweep voltametry of NiO/Ni-CNT, Pt/C deposited on Ni foam (under a loading of 8 mg/cm^2) and pure Ni foam at a scan rate of 1 mV/s in 1 M KOH. (b) Linear sweep voltametry of water electrolysis using NiO/Ni-CNT as cathode and NiFe LDH as anode (both deposited on Ni foam under the loading of 8 mg/cm^2) in 1 M KOH at different temperatures. (c) Chonopotentiometry of water electrolysis with NiO/Ni-CNT as cathode and NiFe LDH as anode at a constant current density of 20 mA/cm^2 in 1 M KOH under different temperature. (d) Demonstration of a water electrolyzer powered by an AAA battery with a voltage of 1.5 V. Reproduced with permission from Ref. [12], Copyright © 2014 Nature Publishing Group.

have great potential for use in future electrolyzers. Improving the durability of the electrocatalysts could further promote their industrial applications.

OER electrocatalysts can also be used in rechargeable metal–air batteries as the positive electrode for charging the battery. During the charging process, water is oxidized at the positive electrode and metal is deposited (reduced) on the negative electrode, while during the discharging process oxygen is reduced at the positive electrode and metal is dissolved (oxidized) at the negative electrode. One of the most promising rechargeable metal–air batteries is the zinc–air battery, due to its high volumetric energy density along with environmental friendliness, low cost and high safety [90]. The rechargeable zinc–air battery usually operates in concentrated alkaline solution containing dissolved zincate ions, which matches the working region of NiFe-based material for OER electrocatalysis. Therefore, we integrated our NiFe LDH electrocatalyst into a primary zinc–air battery consisting of an oxygen reduction reaction (ORR) electrocatalyst with cobalt oxide/nitrogen-doped carbon nanotubes (CoO/NCNT) [91] as the cathode and zinc foil as the anode to make a tri-electrode rechargeable zinc–air battery [92] (Fig. 9(a)). The battery showed an unprecedented small charge–discharge polarization voltage of ~0.70 V at 20 mA/cm^2, matching the performance of precious metal-based catalysts with Pt/C as ORR catalyst and Ir/C as OER catalyst (Fig. 9(b)). Importantly, a zinc–air battery with NiFe LDH and CoO/NCNT exhibited negligible voltage change or material degradation during both charging and discharging (Figs. 9(c) and 9(d)), while one with Pt/C and Ir/C showed drastic decay over time on the Ir/C side (Fig. 9(c)). Therefore, NiFe-based materials, as promising OER electrocatalysts, can be utilized in advanced energy storage applications such as rechargeable zinc–air batteries.

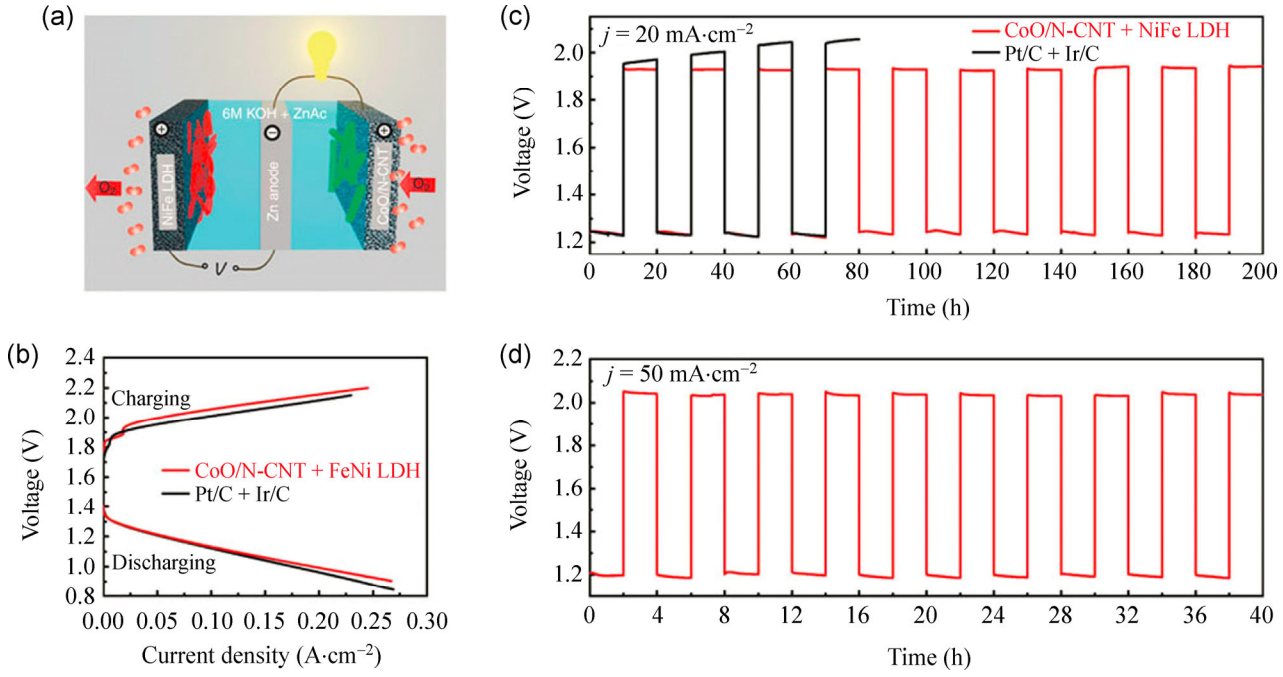

Figure 9 (a) Schematic view of the tri-electrode configuration with CoO/NCNT ORR catalyst loaded on CFP electrode (1 mg/cm^2) and NiFe LDH OER catalyst loaded on Ni foam (~5 mg/cm^2) electrode for discharge and charge, respectively. (b) Charge–discharge polarization curves of the rechargeable Zn–air battery using CoO/NCNT and NiFe LDH (red) compared with one using commercial Pt/C and Ir/C (black). (c) Charge–discharge cycling performance of the rechargeable Zn–air battery using CoO/NCNT and NiFe LDH at 20 mA/cm^2 with a charge–discharge time of 10 h compared with one using Pt/C and Ir/C. (d) Charge–discharge cycling performance of the rechargeable Zn–air battery using CoO/NCNT and NiFe LDH at 50 mA/cm^2 with charge/discharge time of 2 h. Reproduced with permission from Ref. [92], Copyright © 2013 Nature Publishing Group.

10 Conclusions

This review highlights the earlier discovery of, and recent progress with, NiFe-based compounds for oxygen evolution electrocatalysis. OER is a kinetically sluggish reaction that requires electrocatalysts to expedite the reaction, and NiFe-based materials are promising candidates with low cost and high activity in alkaline conditions. Various NiFe compounds with distinct chemical structures, physical morphologies and catalytic properties have been synthesized and investigated. Electrodeposited NiFe alloy films, one of the earliest studied materials, can afford optimal electrical contact with the underlying substrate but show moderate activity and low durability due to the phase transformation necessary prior to OER catalysis. High-temperature annealed NiFe oxides exhibit high durability but relatively low activity due to the highly crystalline phase and chemical stability of mixed NiFe oxides (especially for corrosion-resistant $NiFe_2O_4$). NiFe LDH is a rising candidate with the highest activity, owing to its large electrochemically active surface area, but it still suffers from low electrical conductivity. High throughput screening analysis has also been developed to select advanced NiFe-based materials containing other elements with better performance. Despite tremendous effort, and the progress that has been made in the development of novel NiFe-based materials with better activity and stability, few reports have elaborated the detailed mechanism responsible for the improved activity resulting from Fe incorporation. Mechanistic studies have confirmed the modification of structural and electronic properties after Fe introduction, and a NiOOH-based active phase was indicated by *in situ* spectroscopy. The cause of greatly enhanced OER catalysis after Fe incorporation still remains unclear, and this should be a focus of future studies. Possible approaches might be *in situ* spectroscopy and theoretical calculations with an applied potential. Understanding the basic mechanism could greatly facilitate the discovery of advanced NiFe-based OER

electrocatalysts with higher activity and stability, which will find applications in energy conversion and energy storage applications such as water splitting and rechargeable metal–air batteries.

References

[1] Cook, T. R.; Dogutan, D. K.; Reece, S. Y.; Surendranath, Y.; Teets, T. S.; Nocera, D. G. Solar energy supply and storage for the legacy and non legacy worlds. *Chem. Rev.* **2010**, *110*, 6474–6502.

[2] Gray, H. B. Powering the planet with solar fuel. *Nat. Chem.* **2009**, *1*, 7.

[3] Kudo, A.; Miseki, Y. Heterogeneous photocatalyst materials for water splitting. *Chem. Soc. Rev.* **2009**, *38*, 253–278 .

[4] Lewis, N. S.; Nocera, D. G. Powering the planet: Chemical challenges in solar energy utilization. *Proc. Natl. Acad. Sci. USA* **2006**, *103*, 15729–15735.

[5] Liang, Y. Y.; Li, Y. G.; Wang, H. L.; Dai, H. J. Strongly coupled inorganic/nanocarbon hybrid materials for advanced electrocatalysis. *J. Am. Chem. Soc.* **2013**, *135*, 2013–2036.

[6] Walter, M. G.; Warren, E. L.; Mckone, J. R.; Boettcher, S. W.; Mi, Q. X.; Santori, E. A.; Lewis, N. S. Solar water splitting cells. *Chem. Rev.* **2010**, *110*, 6446–6473.

[7] Wang, H. L.; Dai, H. J. Strongly coupled inorganic-nano-carbon hybrid materials for energy storage. *Chem. Soc. Rev.* **2013**, *42*, 3088–3113.

[8] Crabtree, G. W.; Dresselhaus, M. S.; Buchanan, M. V. The hydrogen economy. *Phys Today* **2004**, *57*, 39–44.

[9] Dresselhaus, M. S.; Thomas, I. L. Alternative energy technologies. *Nature* **2001**, *414*, 332–337.

[10] Choi, C. L.; Feng, J.; Li, Y. G.; Wu, J.; Zak, A.; Tenne, R. WS_2 nanoflakes from nanotubes for electrocatalysis. *Nano Res.* **2013**, *6*, 921–928.

[11] Carmo, M.; Fritz, D. L.; Merge, J.; Stolten, D. A comprehensive review on PEM water electrolysis. *Int. J. Hydrogen Energy* **2013**, *38*, 4901–4934.

[12] Gong, M.; Zhou, W.; Tsai, M. C.; Zhou, J. G.; Guan, M. Y.; Lin, M. C.; Zhang, B.; Hu, Y. F.; Wang, D. Y.; Jiang, J. Nanoscale nickel oxide/nickel heterostructures for active hydrogen evolution electrocatalysis. *Nat. commun.* **2014**, *5*, 4695.

[13] Holladay, J. D.; Hu, J.; King, D. L.; Wang, Y. An overview of hydrogen production technologies. *Catal. Today* **2009**, *139*, 244–260.

[14] Zeng, K.; Zhang, D. K. Recent progress in alkaline water electrolysis for hydrogen production and applications. *Prog. Energ. Combust.* **2010**, *36*, 307–326.

[15] Wu, J.; Xue, Y.; Yan, X.; Yan, W. S.; Chen, Q. M.; Xie, Y. Co_3O_4 nanocrystals on single-walled carbon nanotubes as a highly efficient oxygen-evolving catalyst. *Nano Res.* **2012**, *5*, 521–530.

[16] Tueysuez, H.; Hwang, Y. J.; Khan, S. B.; Asiri, A. M.; Yang, P. Mesoporous Co_3O_4 as an electrocatalyst for water oxidation. *Nano Res.* **2013**, *6*, 47–54.

[17] Dau, H.; Limberg, C.; Reier, T.; Risch, M.; Roggan, S.; Strasser, P. The mechanism of water oxidation: From electrolysis via homogeneous to biological catalysis. *Chemcatchem* **2010**, *2*, 724–761.

[18] Jiao, F.; Frei, H. Nanostructured cobalt and manganese oxide clusters as efficient water oxidation catalysts. *Energ. Environ. Sci.* **2010**, *3*, 1018–1027.

[19] Mills, A. Heterogeneous redox catalysts for oxygen and chlorine evolution. *Chem. Soc. Rev.* **1989**, *18*, 285–316.

[20] Yagi, M.; Kaneko, M. Molecular catalysts for water oxidation. *Chem. Rev.* **2001**, *101*, 21–35.

[21] Kanan, M. W.; Nocera, D. G. *In situ* formation of an oxygen-evolving catalyst in neutral water containing phosphate and Co^{2+}. *Science* **2008**, *321*, 1072–1075.

[22] Koper, M. T. M. Thermodynamic theory of multi–electron transfer reactions: Implications for electrocatalysis. *J. Electroanal. Chem.* **2011**, *660*, 254–260.

[23] Lee, Y.; Suntivich, J.; May, K. J.; Perry, E. E.; Shao-Horn, Y. Synthesis and activities of rutile IrO_2 and RuO_2 nanoparticles for oxygen evolution in acid and alkaline solutions. *J. Phys. Chem. Lett.* **2012**, *3*, 399–404.

[24] McCrory, C. C. L.; Jung, S.; Peters, J. C.; Jaramillo, T. F. Benchmarking heterogeneous electrocatalysts for the oxygen evolution reaction. *J. Am. Chem. Soc.* **2013**, *135*, 16977–16987.

[25] Over, H. Surface chemistry of Ruthenium dioxide in heterogeneous catalysis and electrocatalysis: From fundamental to applied research. *Chem. Rev.* **2012**, *112*, 3356–3426.

[26] Foerster, F.; Piguet, A. On the understanding of anodic formation of oxygen. *Z. Angew. Phys. Chem.* **1904**, *10*, 714–721.

[27] Seiger, H. N.; Shair, R. C. Oxygen evolution from heavily doped nikel oxide electrodes. *J. Electrochem. Soc.* **1961**, *108*, C163.

[28] Tichenor, R. L. Nickel oxides relation between electrochemical reactivity and foreign ion content. *Ind. Eng. Chem.* **1952**, *44*, 973–977.

[29] Troilius, G.; Alfelt, G. The migration of iron in alkaline nickel–cadmium cells with pocket electrodes. *Proceedings of the Fifth International Symposium on Power Sources*, Brighton, UK, 1967. pp 337–348.

[30] Falk, S. U.; Salkind, A. J. *Alkaline storage batteries*. Wiley: New York, 1969.

[31] Munshi, M. Z. A.; Tseung, A. C. C.; Parker, J. The dissolution of iron from the negative material in pochet plate nickel cadmium batteries. *J. Appl. Electrochem.* **1985**, *15*, 711–717.

[32] Hickling, A.; Hill, S. Oxygen overvoltage. 1. The influence of electrode material, current density, and time in aqueous solution. *Discuss. Faraday. Soc.* **1947**, *1*, 236–246.

[33] Cordoba, S. I.; Carbonio, R. E.; Teijelo, M. L.; Macagno, V. A. The effect of the preparation method of mixed nickel iron hydroxide electrodes on the oxygen evolution reaction. *J. Electrochem. Soc.* **1986**, *133*, C300.

[34] Corrigan, D. A. The catalysis of the oxygen evolution reaction by iron impurities in thin-film nickel-oxide electrodes. *J. Electrochem. Soc.* **1987**, *134*, 377–384.

[35] Mlynarek, G.; Paszkiewicz, M.; Radniecka, A.The effect of ferric ions on the behavior of a nickelous hydroxide electrode. *J. Appl. Electrochem.* **1984**, *14*, 145–149.

[36] Hall, D. E. Electrodes for alkaline water electrolysis. *J. Electrochem. Soc.* **1981**, *128*, 740–746.

[37] Bowen, C. T.; Davis, H. J.; Henshaw, B. F.; Lachance, R.; Leroy, R. L.; Renaud, R. Developments in advanced alkaline water electrolysis. *Int. J. Hydrogen Energ.* **1984**, *9*, 59–66.

[38] Janjua, M. B. I.; Leroy, R. L. Electrocatalyst performance in industrial water electrolysers. *Int. J. Hydrogen Energ.* **1985**, *10*, 11–19.

[39] Birss, V. I.; Damjanovic, A.; Hudson, P. G. Oxygen evolution at platinum electrodes in alkaline solutions. 2.Mechanism of the reaction. *J. Electrochem. Soc.* **1986**, *133*, 1621–1625.

[40] Conway, B. E.; Liu, T. C. Characterization of electrocatalysis in the oxygen evolution reaction at platinum by evolution of behavior of surface intermediate states at the oxide film. *Langmuir* **1990**, *6*, 268–276.

[41] Corrigan, D. A.; Bendert, R. M. Effect of coprecipitated metal-ions on the electrochemistry of nickel-hydroxide thin-films-cyclic voltammetry in 1M KOH. *J. Electrochem. Soc.* **1988**, *135*, C156.

[42] Kleinke, M. U.; Knobel, M.; Bonugli, L. O.; Teschke, O. Amorphous alloys as anodic and cathodic materials for alkaline water electrolysis. *Int. J. Hydrogen Energ.* **1997**, *22*, 759–762.

[43] Plata-Torres, M.; Torres-Huerta, A. M.; Dominguez-Crespo, M. A.; Arce-Estrada, E. M.; Ramirez-Rodriguez, C. Electrochemical performance of crystalline Ni-Co-Mo-Fe electrodes obtained by mechanical alloying on the oxygen evolution reaction. *Int. J. Hydrogen Energ.* **2007**, *32*, 4142–4152.

[44] Potvin, E.; Brossard, L. Electrocatalytic activity of Ni-Fe anodes for alkaline water electrolysis. *Mater. Chem. Phys.* **1992**, *31*, 311–318.

[45] Singh, R. N.; Pandey, J. P.; Anitha, K. L. Preparation of electrodeposited thin-films of nickel iron-alloys on mild-steel for alkaline water electrolysis. 1. Studies on oxygen evolutiont. *Int. J. Hydrogen Energ.* **1993**, *18*, 467–473.

[46] Grande, W. C.; Talbot, J. B. Electrodeposition of thin-films of nickel-iron.1. Experimental. *J. Electrochem. Soc.* **1993**, *140*, 669–674.

[47] Solmaz, R.; Kardas, G. Electrochemical deposition and characterization of NiFe coatings as electrocatalytic materials for alkaline water electrolysis. *Electrochim. Acta* 2009, **54**, 3726–3734.

[48] Hu, C. C.; Wu, Y. R. Bipolar performance of the electroplated iron-nickel deposits for water electrolysis. *Mater. Chem. Phys.* **2003**, *82*, 588–596.

[49] Ullal, Y.; Hegde, A. C. Electrodeposition and electrocatalytic study of nanocrystalline Ni-Fe alloy. *Int. J. Hydrogen Energ.* **2014**, *39*, 10485–10492.

[50] Li, X.; Walsh, F. C.; Pletcher, D. Nickel based electrocatalysts for oxygen evolution in high current density, alkaline water electrolysers. *Phys. Chem. Chem. Phys.* **2011**, *13*, 1162–1167.

[51] Perez-Alonso, F. J.; Adan, C.; Rojas, S.; Pena, M. A.; Fierro, J. L. G. Ni/Fe electrodes prepared by electrodeposition method over different substrates for oxygen evolution reaction in alkaline medium. *Int. J. Hydrogen Energ.* **2014**, *39*, 5204–5212.

[52] Kleiman-Shwarsctein, A.; Hu, Y.-S.; Stucky, G. D.; McFarland, E. W. NiFe-oxide electrocatalysts for the oxygen evolution reaction on Ti doped hematite photoelectrodes. *Electrochem. Commun.* **2009**, *11*, 1150–1153.

[53] Louie, M. W.; Bell, A. T. An investigation of thin-film Ni-Fe oxide catalysts for the electrochemical evolution of oxygen. *J. Am. Chem. Soc.* **2013**, *135*, 12329–12337.

[54] Merrill, M. D.; Dougherty, R. C. Metal oxide catalysts for the evolution of O_2 from H_2O. *J. Phys. Chem. C* **2008**, *112*, 3655–3666.

[55] Kim, K. H.; Zheng, J. Y.; Shin, W.; Kang, Y. S. Preparation of dendritic NiFe films by electrodeposition for oxygen evolution. *RSC Adv.* **2012**, *2*, 4759–4767 .

[56] Singh, R. N.; Singh, J. P.; Lal, B.; Thomas, M. J. K.; Bera, S. New $NiFe_{2-x}Cr_xO_4$ spinel films for O_2 evolution in alkaline solutions. *Electrochim Acta* **2006**, *51*, 5515–5523.

[57] Anindita, A.; Singh, R. N. Effect of V substitution at B-site on the physicochemical and electrocatalytic properties of spinel-type $NiFe_2O_4$ towards O_2 evolution in alkaline solutions. *Int. J.Hydrogen Energ.* **2010**, *35*, 3243–3248.

[58] Kumar, M.; Awasthi, R.; Sinha, A. S. K.; Singh, R. N. New ternary Fe, Co, and Mo mixed oxide electrocatalysts for oxygen evolution. *Int. J. Hydrogen Energ.* **2011**, *36*, 8831–8838.

[59] Chanda, D.; Hnat, J.; Paidar, M.; Bouzek, K. Evolution of physicochemical and electrocatalytic properties of $NiCo_2O_4$ (AB(2)O(4)) spinel oxide with the effect of Fe substitution

at the A site leading to efficient anodic O_2 evolution in an alkaline environment. *Int. J. Hydrogen Energ.* **2014**, *39*, 5713–5722.

[60] Cheng, Y.; Liu, C.; Cheng, H.-M.; Jiang, S. P. One-pot synthesis of metal-carbon nanotubes network hybrids as highly efficient catalysts for oxygen evolution reaction of water splitting. *ACS Appl. Mater. Inter.* **2014**, *6*, 10089–10098.

[61] Singh, N. K.; Singh, R. N. Electrocatalytic properties of spinel type $Ni_xFe_{3-x}O_4$ synthesized at low temperature for oxygen evolution in KOH solutions. *Indian J. Chem. Sect A–Inorg. Bio–Inorg. Phys. Theor. Anal. Chem.* **1999**, *38*, 491–495.

[62] Trotochaud, L.; Ranney, J. K.; Williams, K. N.; Boettcher, S. W. Solution-cast metal oxide thin film electrocatalysts for oxygen evolution. *J. Am. Chem. Soc.* **2012**, *134*, 17253–17261.

[63] Lu, Z. Y.; Wang, H. T.; Kong, D. S.; Yan, K.; Hsu, P. C.; Zheng, G. Y.; Yao, H. B.; Liang, Z.; Sun, X. M.; Cui, Y. Electrochemical tuning of layered lithium transition metal oxides for improvement of oxygen evolution reaction. *Nat.Commun.* **2014**, *5*, 4345.

[64] Miller, E. L.; Rocheleau, R. E. Electrochemical behavior of reactively sputtered iron-doped nickel oxide. *J. Electrochem. Soc.* **1997**, *144*, 3072–3077.

[65] Kodama, R. H.; Berkowitz, A. E.; McNiff, E. J.; Foner, S. Surface spin disorder in $NiFe_2O_4$ nanoparticles. *Phys. Rev. Lett.* **1996**, *77*, 394–397.

[66] Kodama, R. H. Magnetic nanoparticles. *J. Magn. Magn. Mater.* **1999**, *200*, 359–372.

[67] Smith, R. D. L.; Prevot. M. S.; Fagan, R. D.; Zhang, Z. P.; Sedach, P. A.; Sui, M. K. J.; Trudel, S.; Berlinguette, C. P. Photochemical route for accessing amorphous metal oxide materials for water oxidation catalysis. *Science* **2013**, *340*, 60–63.

[68] Evans, D. G.; Slade, R. C. T. Structural aspects of layered double hydroxides. In *Layered Double Hydroxides*, Vol. 119. X. Duan & D. G. Evans, eds. Springer: Berlin, Heidelberg, New York, 2006.

[69] Wang, Q.; O'Hare, D. Recent advances in the synthesis and application of layer double hydroxide (LDH) Nanosheets. *Chem. Rev.* **2012**, *112*, 4124–4155.

[70] Fan, G. L.; Li, F.; Evans, D. G.; Duan, X. Catalytic applications of layered double hydroxides: Recent advances and perspectives. *Chem. Soc. Rev.* **2014**, *43*, 7040–7066.

[71] Refait, P.; Abdelmoula, M.; Simon, L.; Genin, J. M. R. Mechanisms of formation and transformation of Ni-Fe layered double hydroxides in SO^{2-} and SO_4^{2-} containing aqueous solutions. *J. Phys. Chem. Solids* **2005**, *66*, 911–917.

[72] Shi, Q. X.; Lu, R. W.; Lu, L. H.; Fu, X. M.; Zhao, D. F. Efficient reduction of nitroarenes over nickel-iron mixed oxide catalyst prepared from a nickel-iron hydrotalcite precursor. *Adv. Synth. Catal.* **2007**, *349*, 1877–1881.

[73] Gong, M.; Li, Y. G.; Wang, H. L.; Liang, Y. Y.; Wu, J. Z.; Zhou, J. G.; Wang, J.; Rieger, T.; Wei, F.; Dai, H. J. An advanced Ni-Fe layered double hydroxide electrocatalyst for water oxidation. *J. Am. Chem. Soc.* **2013**, *135*, 8452–8455.

[74] Long, X.; Li, J. K.; Xiao, S.; Yan, K. Y.; Wang, Z. L.; Chen, H. N.; Yang, S. H. A strongly coupled graphene and FeNi double hydroxide hybrid as an excellent electrocatalyst for the oxygen evolution reaction. *Angew. Chem. Int. Ed.* **2014**, *53*, 7584–7588.

[75] Tang, D.; Liu, J.; Wu, X. Y.; Liu, R. H.; Han, X.; Han, Y. Z.; Huang, H.; Liu, Y.; Kang, Z. H. Carbon quantum dot/NiFe layered double-hydroxide composite as a highly efficient electrocatalyst for water oxidation. *ACS Appl. Mater. Inter.* **2014**, *6*, 7918–7925.

[76] Lu, Z. Y.; Xu, W. W.; Zhu, W.; Yang, Q.; Lei, X. D.; Liu, J. F.; Li, Y. P.; Sun, X. M.; Duan, X. Three-dimensional NiFe layered double hydroxide film for high-efficiency oxygen evolution reaction. *Chem. Commun.* **2014**, *50*, 6479–6482.

[77] Trotochaud, L.; Young, S. L.; Ranney, J. K.; Boettcher, S. W. Nickel-iron oxyhydroxide oxygen-evolution electrocatalysts: The role of intentional and incidental iron incorporation. *J. Am. Chem. Soc.* **2014**, *136*, 6744–6753.

[78] Song, F.; Hu, X. L. Exfoliation of layered double hydroxides for enhanced oxygen evolution catalysis. *Nat. commun.* **2014**, *5*, 4477.

[79] Gerken, J. B.; Chen, J. Y. C.; Masse, R. C.; Powell, A. B.; Stahl, S. S. Development of an O_2-sensitive fluorescence-quenching assay for the combinatorial discovery of electrocatalysts for water oxidation. *Angew. Chem.Inter. Ed.* **2012**, *51*, 6676–6680.

[80] Gerken, J. B.; Shaner, S. E.; Masse, R. C.; Porubsky, N. J.; Stahl, S. S. A survey of diverse earth abundant oxygen evolution electrocatalysts showing enhanced activity from Ni–Fe oxides containing a third metal. *Energ. Environ Sci.* **2014**, *7*, 2376–2382.

[81] Haber, J. A.; Xiang, C. C.; Guevarra, D.; Jung, S. H.; Jin, J.; Gregoire, J. M. High-throughput mapping of the electrochemical properties of $(Ni\text{-}Fe\text{-}Co\text{-}Ce)O_x$ oxygen-evolution catalysts. *Chemelectrochem* **2014**, *1*, 524–528.

[82] Chen, J. Y. C.; Miller, J. T.; Gerken, J. B.; Stahl, S. S. Inverse spinel $NiFeAlO_4$ as a highly active oxygen evolution electrocatalyst: Promotion of activity by a redox-inert metal ion. *Energ. Environ. Sci.* **2014**, *7*, 1382–1386.

[83] Bode, H.; Dehmelt, K.; Witte, J. Nickel hydroxide electrodes. 2. oxidation products of nickel(II) hydroxides. *Z. Anorg. Allg. Chem* **1969**, *366*, 1.

[84] Barnard, R.; Randell, C. F.; Tye, F. L. Studies concerning charged nickel-hydroxide electrodes. 1. Measurements of reversible potentials. *J. Appl. Electrochem.* **1980**, *10*, 109–125.

[85] Lu, P. W. T.; Srinivasan, S. Electrochemical–ellipsometric studies of oxide film for medon nickel during oxygen evolution. *J. Electrochem. Soc.* **1978**, *125*, 1416–1422.

[86] Lyons, M. E. G.; Brandon, M. P. The oxygen evolution reaction on passive oxide covered transition metal electrodes in aqueous alkaline solution. Part 1–Nickel. *Inter. J. Electrochem. Sci.* **2008**, *3*, 1386–1424.

[87] Bediako, D. K.; Lassalle-Kaiser, B.; Surendranath, Y.; Yano, J.; Yachandra, V. K.; Nocera, D. G. Structure-activity correlations in a nickel–borate oxygen evolution catalyst. *J. Am. Chem. Soc.* **2012**, *134*, 6801–6809.

[88] Landon, J.; Demeter, E.; Inoglu, N.; Keturakis, C.; Wachs, I. E.; Vasic, R.; Frenkel, A. I.; Kitchin, J. R. Spectroscopic characterization of mixed Fe–Ni oxide electrocatalysts for the oxygen evolution reaction in alkaline electrolytes. *ACS Catal.* **2012**, *2*, 1793–1801.

[89] Li, Y.-F.; Selloni, A. Mechanism and activity of water oxidation on selected surfaces of pure and Fe-doped NiO_x. *ACS Catal.* **2014**, *4*, 1148–1153.

[90] Li, Y. G.; Dai, H. J. Recent advances in zinc-air batteries. *Chem. Soc. Rev.* **2014**, *43*, 5257.

[91] Liang, Y. Y.; Wang, H. L.; Diao, P.; Chang, W.; Hong, G. S.; Li, Y. G.; Gong, M.; Xie, L. M.; Zhou, J. G.; Wang, J. Oxygen reduction electrocatalyst based on strongly coupled cobalt oxide nanocrystals and carbon nanotubes. *J. Am. Chem. Soc.* **2012**, *134*, 15849–15857.

[92] Li, Y. G.; Gong, M.; Liang, Y. Y.; Feng, J.; Kim, J. E.; Wang, H. L.; Hong, G. S.; Zhang, B.; Dai, H. J. Advanced zinc-air batteries based on high-performance hybrid electrocatalysts. *Nat. commun* **2013**, **4**.